Paper 58

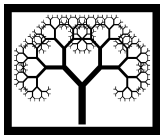

Proceedings of the Eleventh International Conference
on Computational Structures Technology,
B.H.V. Topping, (Editor),
Civil-Comp Press, Stirlingshire, Scotland

Sequentially Linear Analysis applied to a FETI-Based Model of Quasi-Brittle Interfaces

P. Gruber and J. Zeman
Department of Mechanics, Faculty of Civil Engineering
Czech Technical University in Prague, Czech Republic

Abstract

This paper introduces a robust numerical tool for the modelling of brittle and quasi-brittle interfaces. Such interfaces are characterised by a rapid dissipation of a reversible stored energy which is commonly accompanied by the so-called snap-back phenomenon. It leads to numerical instability of standard mathematical approaches. The small-strain setting model presented is subservient to quasistatic processes and individual linear elastic domains are joined by (quasi-)brittle friction-less interfaces. The method of local state is adopted and a current internal interface state is defined by one internal variable, the well-known scalar damage parameter. A formal energetic formulation of problem is solved using the sequential linear analysis (SLA). The common discretization of problem by primal variant of finite element method (FEM) is substituted by the finite element tearing and interconnecting (FETI) method. Finally, numerical experiment on a layered beam is introduced.

Keywords: damage, energetic solution, FETI, local state method, quasi-brittle interfaces, sequentially linear analysis, snap-back.

1 Introduction

It is generally accepted that the key factor the governing mechanical performance in heterogeneous structures (laminated beams, sandwich structures, etc.) is the interfacial debonding due damage processes active at the constituents' interfaces [1]. In this contribution, we introduce an efficient energy- and duality-based approach to the numerical modelling of heterogeneous materials and structures with imperfect quasi-brittle interfaces.

Although the majority of computational works in the field employ the primal, displacement-based, variant of the finite element method (FEM), its application to

imperfectly bonded assemblies suffers from specific difficulties. In particular, an interface is introduced into the model in the form of an inelastic cohesive element [2], characterized by a finite value of interfacial stiffness. In order to correctly reproduce the perfect interfaces, the stiffness needs to be very large, which manifests in spurious traction oscillations and hence inaccurate prediction of damage initiation [3]. A low stiffness value, on the other hand, allows for mutual interpenetration of individual constituents, resulting in a non-physical distribution of mechanical fields. Furthermore, it is now well-understood that an efficient treatment of contact among adjacent domains, even for the frictionless approximation, is relatively difficult in the framework of primal FEM techniques [4].

Our approach attempts to eliminate the above mentioned problems. It is a rate-independent energy-based model which uses the principles of isotropic damage mechanics to model the evolution of interfacial damage [5]. A mixed-mode constitutive model with linear softening is implemented, based on the developments of Geubelle and Baylor [6] and Ortiz and Pandolfi [7].

The continuous formulation is approximated by Sequence of linear analyses, which is subsequently discretized using the FEM method. The problem is converted into the dual form, expressed in terms of interfacial forces that enforce the displacement compatibility. For the perfect bonding case, the resulting system is equivalent to the original Finite Element Tearing and Interconnecting (FETI) method due to Farhat and Roux [8]. For imperfect interfaces, we recover modified FETI equations first proposed by Kruis and Bittnar [9], which are complemented with a simple projection technique to ensure the frictionless contact conditions. In both cases, the system is well-suited for the treatment by Preconditioned Conjugate Gradient algorithm, see [10] for additional details.

The remainder of the paper is organized as follows. In Section 2, we introduce geometrical description, state variables and all energy functionals related to the rate-independent system. Section 3 introduces the notion of the energetic solution and the sequentially linear analysis. The numerical treatment of this variational problem is outlined in Section 4, with emphasis given to the derivation of the FETI-based optimality conditions in Section 5. Finally, the model is validated by force-displacement diagrams of two-layer laminated beam subject to mode-II conditions.

2 Model Setup

We start from introducing the continuous version of the energy-based delamination model closely following the exposition of Kočvara et.al [5]. For simplicity, we restrict our attention to the small-strain setting and assume that inelastic processes are concentrated to interfaces only, whereas the bulk response remains elastic.

2.1 Geometrical description

We consider a system of n disjoint bodies, represented by open domains $\Omega^{(i)} \subset \mathbb{R}^{\mathrm{d}}$, $d \in \{2, 3\}$, with boundaries $\Gamma^{(i)} := \partial\Omega^{(i)}$, where $i \in \{1, 2, \ldots, n\}$. The closure of the i-th domain is denoted as $\bar{\Omega}^{(i)} := \Omega^{(i)} \cup \Gamma^{(i)}$. The (possibly empty) common boundary between two bodies $\Omega^{(i)}$ and $\Omega^{(j)}$ will be defined by $\Gamma^{(i)}_j := \bar{\Omega}^{(i)} \cap \bar{\Omega}^{(j)}$, with $i < j$ and $j \in \{1, 2, \ldots, n\}$.

It will also be useful to distinguish internal interfaces of the system

$$\Gamma^{(i)}_{\mathrm{int}} := \bigcup_{j=i+1}^{n} \Gamma^{(i)}_j, \qquad \Gamma_{\mathrm{int}} := \bigcup_{i=1}^{n} \Gamma^{(i)}_{\mathrm{int}} \tag{1}$$

from the external boundary $\Gamma := \partial\Omega \setminus \Gamma_{\mathrm{int}}$, where

$$\Omega := \bigcup_{i=1}^{n} \Omega^{(i)}. \tag{2}$$

At each material point $\boldsymbol{x}$ on a non-empty interface $\Gamma^{(i)}_j$, a local Cartesian coordinate system is introduced in terms of its origin $\boldsymbol{x}$ and unit vectors

$$\left\{ \boldsymbol{n}^{(i)}(\boldsymbol{x}), \boldsymbol{t}^{(i)}_1(\boldsymbol{x}), \ldots, \boldsymbol{t}^{(i)}_{d-1}(\boldsymbol{x}) \right\}$$

aligned with its axes; the symbols $\boldsymbol{n}^{(i)}(\boldsymbol{x})$ and $\boldsymbol{t}^{(i)}_j(\boldsymbol{x})$ denote the outer normal and j-th tangential vectors to the boundary, respectively. Note that in what follows, all interface-related quantities will be defined in this local coordinate system.

2.2 State Variables

Two fields of the observable state variables are used for characterization of an introduced system state: (i) domain displacements $\boldsymbol{u}^{(i)} : \Omega^{(i)} \to \mathbb{R}^{\mathrm{d}}$ and (ii) interfacial displacement jumps $[\![\boldsymbol{u}]\!] : \Gamma_{\mathrm{int}} \to \mathbb{R}^{\mathrm{d}}$. Next, there is only one internal variable – the well-known damage parameter $\omega : \Gamma_{\mathrm{int}} \to \mathbb{R}$.

2.3 Admissible Fields

An admissible domain displacement $\hat{\boldsymbol{u}}(\boldsymbol{x})^{(i)}$ is constrained to

$$\mathbb{K}^{(i)} := \left\{ \hat{\boldsymbol{u}}^{(i)}(\boldsymbol{x}) : \hat{\boldsymbol{u}}^{(i)}|_{\Gamma^{(i)}}(\boldsymbol{x}) = \boldsymbol{u}_{\mathrm{D}}(\boldsymbol{x}), \forall \boldsymbol{x} \in \Gamma_{\mathrm{D}} \cap \Gamma^{(i)} \right\}, \tag{3}$$

where $\boldsymbol{u}_{\mathrm{D}}$ denotes the prescribed displacements on the Dirichlet part of the external boundary $\Gamma_{\mathrm{D}} \subset \Gamma$.

Further, we introduce the split of the interfacial displacement jumps to the normal and tangential components in the form

$$[\![\hat{u}]\!]_{\mathrm{n}}(\boldsymbol{x}) := [\![\hat{\boldsymbol{u}}]\!](\boldsymbol{x}) \cdot \boldsymbol{n}^{(i)}(\boldsymbol{x}), \qquad [\![\hat{\boldsymbol{u}}]\!]_{\mathrm{t}}(\boldsymbol{x}) := [\![\hat{\boldsymbol{u}}]\!](\boldsymbol{x}) - [\![\hat{u}]\!]_{\mathrm{n}}(\boldsymbol{x})\, \boldsymbol{n}^{(i)}(\boldsymbol{x}) \tag{4}$$

for all $\boldsymbol{x} \in \Gamma_{\text{int}}^{(i)}$ and $i = \{1, 2, \ldots, n\}$. Denoting collectively the domain displacements as $\hat{\boldsymbol{u}}(\boldsymbol{x}) := \left(\hat{\boldsymbol{u}}^{(i)}(\boldsymbol{x})\right)_{i=1}^{n}$, the set of admissible displacement jumps receives the form

$$\begin{aligned}\mathbb{K}^{[\![u]\!]}\left(\hat{\boldsymbol{u}}(\boldsymbol{x})\right) \;=\; & \Big\{ [\![\hat{\boldsymbol{u}}]\!]_{\text{n}}(\boldsymbol{x}) \geq 0 : \forall \boldsymbol{x} \in \Gamma_{\text{int}}, \\ & [\![\hat{\boldsymbol{u}}]\!](\boldsymbol{x}) = \boldsymbol{T}_j^{(i)}(\boldsymbol{x}) \left(\hat{\boldsymbol{u}}^{(i)}|_{\Gamma_j^{(i)}}(\boldsymbol{x}) - \hat{\boldsymbol{u}}^{(j)}|_{\Gamma_j^{(i)}}(\boldsymbol{x})\right) : \forall \boldsymbol{x} \in \Gamma_j^{(i)}, \\ & j \in \{1, 2, \ldots, n\}, i < j \Big\}. \end{aligned} \tag{5}$$

The first condition in (5) enforces the interpenetration among adjacent bodies, whereas the later equality ensures the kinematic compatibility between displacement jumps and domain displacements, converted into the local coordinate system using matrices $\boldsymbol{T}_j^{(i)}$.

Finally, we introduce an admissible set of the internal variable

$$\mathbb{W} := \{\hat{\omega}(\boldsymbol{x}) : \hat{\omega}(\boldsymbol{x}) \in [0; 1], \forall \boldsymbol{x} \in \Gamma_{\text{int}}\}, \tag{6}$$

where $\hat{\omega}(\boldsymbol{x}) = 0$ corresponds with a perfect interface and $\hat{\omega}(\boldsymbol{x}) = 1$ indicates a fully damaged interfacial material point.

2.4 Interfacial constitutive law

The inelastic interfacial behavior is described by means of scalar damage law with linear softening, cf. [6, 7]. In the one-dimensional version, the interface is characterized by the fracture toughness of a perfect interface $G_{c,0}$ (in Jm^{-2}), its critical opening Δ (in m) and the initial damage ω_0, controlling the initial interfacial stiffness. These can be directly related to fracture toughness G_c and strength $\sigma_{\max}$ (in Pa) of an elastic-damaging representation

$$G_c = (1 - \omega_0) G_{c,0}, \qquad \sigma_{\max} = \frac{1}{2}(1 - \omega_0) G_{c,0} \Delta. \tag{7}$$

The mixed-mode extension is based on an effective displacement jump measure

$$\hat{\delta}\left(\boldsymbol{x}, [\![\hat{\boldsymbol{u}}]\!](\boldsymbol{x})\right) = \sqrt{[\![\hat{\boldsymbol{u}}]\!]_{\text{n}}^2(\boldsymbol{x}) + \beta^2(\boldsymbol{x}) [\![\hat{\boldsymbol{u}}]\!]_{\text{t}}^2(\boldsymbol{x})}, \qquad [\![\hat{\boldsymbol{u}}]\!]_{\text{t}}(\boldsymbol{x}) = \| [\![\hat{\boldsymbol{u}}]\!]_{\text{t}}(\boldsymbol{x}) \|, \tag{8}$$

in which β denotes a mode-mixity parameter determined from experiments.

Notice that $\hat{\delta}(\boldsymbol{x})$ is based on the admissible displacement jumps $\mathbb{K}^{[\![u]\!]}$.

2.5 Energetic Functionals

In accordance with Section 2.4, a density of an elastic energy, reversibility stored at a material interface point $\boldsymbol{x}$, is given by

$$e^{\text{int}}\left(\boldsymbol{x}, \hat{\omega}(\boldsymbol{x}), [\![\hat{\boldsymbol{u}}]\!](\boldsymbol{x})\right) := \frac{G_{c,0}(\boldsymbol{x})}{\Delta^2(\boldsymbol{x})} \frac{1 - \hat{\omega}(\boldsymbol{x})}{\hat{\omega}(\boldsymbol{x})} \hat{\delta}^2\left(\boldsymbol{x}, [\![\hat{\boldsymbol{u}}]\!](\boldsymbol{x})\right) \tag{9}$$

yielding its interfacial counterpart in the form

$$\mathcal{E}^{\mathrm{int}}\left(\hat{\omega}\left(\boldsymbol{x}\right),\hat{[\![\boldsymbol{u}]\!]}\left(\boldsymbol{x}\right)\right):=\int_{\Gamma_{\mathrm{int}}}e^{\mathrm{int}}\left(\boldsymbol{x},\hat{\omega}\left(\boldsymbol{x}\right),\hat{[\![\boldsymbol{u}]\!]}\left(\boldsymbol{x}\right)\right)\mathrm{d}\Gamma. \tag{10}$$

The irreversible processes are characterized by a dissipated energy density

$$d\left(\boldsymbol{x},\hat{\omega}_1\left(\boldsymbol{x}\right),\hat{\omega}_2\left(\boldsymbol{x}\right)\right)=\begin{cases} G_{c,0}\left(\boldsymbol{x}\right)\left(\hat{\omega}_2\left(\boldsymbol{x}\right)-\hat{\omega}_1\left(\boldsymbol{x}\right)\right) & \text{if} \quad \hat{\omega}_1\left(\boldsymbol{x}\right)\leq\hat{\omega}_2\left(\boldsymbol{x}\right) \\ +\infty & \text{otherwise} \end{cases}, \tag{11}$$

due to the change of damage parameter $\hat{\omega}_1$ from to $\hat{\omega}_2$. The $+\infty$' term in (11) enforces unidirectionality of the damage process, i.e. the damaged interface cannot heal (the second thermodynamics law).

The related interfacial dissipation distance is obtained by

$$\mathcal{D}\left(\hat{\omega}_1\left(\boldsymbol{x}\right),\hat{\omega}_2\left(\boldsymbol{x}\right)\right)=\int_{\Gamma_{\mathrm{int}}}d\left(\boldsymbol{x},\hat{\omega}_1\left(\boldsymbol{x}\right),\hat{\omega}_2\left(\boldsymbol{x}\right)\right)\mathrm{d}\Gamma. \tag{12}$$

As introduced earlier in this section, individual sub-domains $\Omega^{(i)}$ are assumed to remain linearly elastic. The associated energy densities are given by

$$e^{(i)}\left(\boldsymbol{x},\hat{\boldsymbol{\epsilon}}^{(i)}\left(\boldsymbol{x}\right)\right)=\frac{1}{2}\hat{\boldsymbol{\epsilon}}^{(i)}:\boldsymbol{C}^{(i)}\left(\boldsymbol{x}\right):\hat{\boldsymbol{\epsilon}}^{(i)}, \tag{13}$$

where $\hat{\boldsymbol{\epsilon}}^{(i)}$ is the linearized strain and $\boldsymbol{C}^{(i)}\left(\boldsymbol{x}\right)$ is a fourth-order tensor of elastic stiffness. It leads to an energy functional

$$\mathcal{E}^{(i)}\left(\hat{\boldsymbol{u}}^{(i)}\left(\boldsymbol{x}\right)\right)=\int_{\Omega^{(i)}}e^{(i)}\left(\boldsymbol{x},\boldsymbol{\nabla}_{\mathrm{s}}\hat{\boldsymbol{u}}^{(i)}\left(\boldsymbol{x}\right)\right)\mathrm{d}\Omega, \tag{14}$$

where $\boldsymbol{\nabla}_{\mathrm{s}}$ denotes the symmetrized gradient.

The last energy component of the model is given by the potential energy of external forces of the i-th domain, expressed in the form

$$\mathcal{W}^{(i)}\left(t,\hat{\boldsymbol{u}}^{(i)}\left(\boldsymbol{x}\right)\right)=-\int_{\Omega^{(i)}}\hat{\boldsymbol{u}}^{(i)}\left(\boldsymbol{x}\right)\boldsymbol{v}\left(t,\boldsymbol{x}\right)\mathrm{d}\Omega-\int_{\Gamma^{(i)}}\hat{\boldsymbol{u}}^{(i)}\left(\boldsymbol{x}\right)\boldsymbol{t}\left(t,\boldsymbol{x}\right)\mathrm{d}\Gamma, \tag{15}$$

where $\boldsymbol{v}\left(t,\boldsymbol{x}\right)$ are volume external forces and $\boldsymbol{t}\left(t,\boldsymbol{x}\right)$ are surface tractions, given as functions of a pseudo-time $t\in\mathbb{I}:=[0,T]$, where T is positive constatnt.

3 Energetic Solution

The energetic solution is based on two basic requirements. The first one so-called stability inequality (16) which besides the potential energy takes into account also the dissipation. The second requirement so-called energy balance (17) expresses the second law of thermodynamics bysaying that the energy put to the system by external forces or boundary conditions is pent on the change of potential energy and/or on dissipation.

3.1 Global Stability and Energy Balance

For initial data $\boldsymbol{u}^{(i)}(0,\boldsymbol{x})$, $[\![\boldsymbol{u}]\!](0,\boldsymbol{x})$ and $\omega(0,\boldsymbol{x})$, the energetic solution of the rate-independent evolution in pseudo-time $t \in \mathbb{I}$ is provided by functions $\boldsymbol{u}^{(i)}(t,\boldsymbol{x})$, $[\![\boldsymbol{u}]\!](t,\boldsymbol{x})$ and $\omega(t,\boldsymbol{x})$, for all $i \in \{1,2,\ldots,n\}$. The energetic solution satisfies the conditions of the global stability

$$\sum_{i=1}^{n} \mathcal{E}^{(i)}\left(\boldsymbol{u}^{(i)}(t,\boldsymbol{x})\right) + \mathcal{E}^{\mathrm{int}}\left(\omega(t,\boldsymbol{x}), [\![\boldsymbol{u}]\!](t,\boldsymbol{x})\right) - \sum_{i=1}^{n} \mathcal{W}^{(i)}\left(t, \boldsymbol{u}^{(i)}(t,\boldsymbol{x})\right) \leq$$

$$\sum_{i=1}^{n} \mathcal{E}^{(i)}\left(\hat{\boldsymbol{u}}^{(i)}(\boldsymbol{x})\right) + \mathcal{E}^{\mathrm{int}}\left(\hat{\omega}(\boldsymbol{x}), \hat{[\![\boldsymbol{u}]\!]}(\boldsymbol{x})\right) + \mathcal{D}\left(\omega(t,\boldsymbol{x}), \hat{\omega}(\boldsymbol{x})\right) - \sum_{i=1}^{n} \mathcal{W}^{(i)}\left(t, \hat{\boldsymbol{u}}^{(i)}(\boldsymbol{x})\right) \quad (16)$$

and the energy balance

$$\sum_{i=1}^{n} \mathcal{E}^{(i)}\left(\boldsymbol{u}^{(i)}(t,\boldsymbol{x})\right) + \mathcal{E}^{\mathrm{int}}\left(\omega(t,\boldsymbol{x}), [\![\boldsymbol{u}]\!](t,\boldsymbol{x})\right) + \mathrm{Var}_D\left(\omega(t,\boldsymbol{x}), [0,t]\right) =$$

$$\sum_{i=1}^{n} \mathcal{E}^{(i)}\left(\boldsymbol{u}^{(i)}(0,\boldsymbol{x})\right) + \mathcal{E}^{\mathrm{int}}\left(\omega(0,\boldsymbol{x}), [\![\boldsymbol{u}]\!](0,\boldsymbol{x})\right) + \sum_{i=1}^{n} \int_0^t \frac{\mathrm{d}}{\mathrm{d}s} \mathcal{W}^{(i)}\left(s, \hat{\boldsymbol{u}}^{(i)}(s,\boldsymbol{x})\right) \mathrm{d}s, \quad (17)$$

where $\mathrm{Var}_D\left(\omega(t,\boldsymbol{x}), [0,t]\right)$ quantifies totally dissipated energy in time interval $[0,t]$.

3.2 Sequentially Linear Analysis

The most natural way for solving of the formal energetic solution defined by conditions (16) and (17) (for mathematically based scientists, especially) leads through time discretization methods, see [11] for more details. Such approach is consistent with a concept developed by mathematics for researching of an evolution in so-called rate independent systems, see [12]. The concept includes mathematically rigorous proofs of solution existence, error estimations, etc.

For more engineered based readers, we offer an alternative approach based on the sequentially linear analysis (SLA) developed by Rots in 2001 (nice review of the method in [13]). The main advantage of the method is an intuitive transparency and robustness (primarily important for the quasi-brittle behaviour), on the other hand, there is not the sophisticated mathematical background.

3.3 Restriction of Admissible Internal States

The SLA selects from the set of admissible internal states $\mathbb{W}$ only a finite number of them – the resulting set is denoted $\mathbb{W}^p$ (the superscript p corresponds with number of selected states). The SLA inserts an order into the set of admissible states $\mathbb{W}$ from a spatial distribution on the interface area Γ_{int} point of view. The discretization of $\mathbb{W}$ to $\mathbb{W}^p \subset \mathbb{W}$, where

$$\mathbb{W}^p = \left\{\hat{\omega}^1(\boldsymbol{x}), \hat{\omega}^2(\boldsymbol{x}), \ldots, \hat{\omega}^p(\boldsymbol{x})\right\}, \quad (18)$$

is based on a sequence of p linear analyses (the word linear is used from the internal state point of view – there is non-linear behaviour induced by the contact problem) supplemented about an incremental dissipation of energy, in k-th linear analysis denoted $\Delta\mathcal{D}^p\left(k\right)$.

For reason of the incremental dissipation, the domain Γ_{int} is subdivided into N_{SLA} simplex subdomains

$$\Gamma_{\mathrm{int}} = \prod_{\alpha=1}^{N_{\mathrm{SLA}}} \Gamma_{\mathrm{SLA}}^{\alpha} \tag{19}$$

and the increment of the dissipation in k-th linear analysis $\Delta\mathcal{D}^p\left(k\right)$ will occur over one of them. Next, in order to unique definition of the increment $\Delta\mathcal{D}^p\left(k\right)$, it is necessary to discretize an internal evolution of a material point state, which can be formally characterized by an auxiliary field $s\left(\boldsymbol{x}\right)$, to q discrete states. Then, a related amount of a dissipated energy density $\Delta d : \{1, 2, \ldots, q\} \times \mathbb{R}^{\mathrm{d}} \rightarrow \mathbb{R}$ have to satisfy

$$G\left(\boldsymbol{x}\right) = \sum_{\hat{s}(x)=1}^{q} \Delta d\left(\hat{s}\left(\boldsymbol{x}\right)\right), \tag{20}$$

where the field $\hat{s} : \Gamma_{\mathrm{int}} \rightarrow \{1, 2, \ldots, q\}$ evaluates discretized internal state of the material point $\boldsymbol{x}$.

3.4 Construction of Admissible Internal States

In this part, a construction of k-th admissible internal state defined by $\hat{\omega}^k\left(\boldsymbol{x}\right) \in \mathbb{W}^p$ and formally defined by $\hat{s}\left(\boldsymbol{x}\right)$ is described. The k-th step of SLA is equivalent to minimization problem

$$\left(\boldsymbol{u}_k\left(\boldsymbol{x}\right), [\![\boldsymbol{u}]\!]_k\left(\boldsymbol{x}\right)\right) = \arg \min_{\left(\hat{\boldsymbol{u}}(\boldsymbol{x}), \hat{[\![\boldsymbol{u}]\!]}(\boldsymbol{x})\right) \in \mathbb{K} \times \mathbb{K}^{[\![u]\!]}} \Phi_k \left(\hat{\boldsymbol{u}}\left(\boldsymbol{x}\right), \hat{[\![\boldsymbol{u}]\!]}\left(\boldsymbol{x}\right), \hat{\omega}^{k-1}\left(\boldsymbol{x}\right)\right), \tag{21}$$

where the associated energetic functional Φ_k is defined as

$$\begin{aligned} \Phi_k \;\; := \;\; & \sum_{i=1}^{n} \mathcal{E}^{(i)}\left(\hat{\boldsymbol{u}}^{(i)}\left(\boldsymbol{x}\right)\right) + \mathcal{E}^{\mathrm{int}}\left(\hat{\omega}^{k-1}\left(\boldsymbol{x}\right), \hat{[\![\boldsymbol{u}]\!]}\left(\boldsymbol{x}\right)\right) \\ - \;\; & \sum_{i=1}^{n} \mathcal{W}^{(i)}\left(1, \hat{\boldsymbol{u}}^{(i)}\left(\boldsymbol{x}\right)\right). \end{aligned} \tag{22}$$

Let exists a state of interfaces $\hat{s}\left(\boldsymbol{x}\right) < q$, then exists a level of reference load defined by pseudo-time t^k such that

$$\left(t^k, \boldsymbol{x}^k\right) = \arg\min\nolimits_{(t,\boldsymbol{x}) \in \mathbb{I} \times \Gamma_{\mathrm{int}}} \frac{\left(1 - \hat{\omega}^{k-1}\left(\boldsymbol{x}\right)\right) Y^*\left(\hat{s}\left(\boldsymbol{x}\right)\right) + \Delta d\left(\hat{s}\left(\boldsymbol{x}\right)\right)}{e^{\mathrm{int}}\left([\![\boldsymbol{u}]\!]_k\left(\boldsymbol{x}\right)\right)}, \tag{23}$$

where $Y^*\left(s\left(\boldsymbol{x}\right)\right)$ denotes the critical driving force whose meaning is energy threshold. In the SLA, until the pseudo-time t^k is reached, no evolution of the internal state

is assumed. On the other side, the achieving of the pseudo-time t^k is joined with incremental change of internal state over all part of interface

$$\Gamma^k_{\mathrm{crit}} = \left\{ \Gamma^\alpha_{\mathrm{SLA}} : \boldsymbol{x}^k \in \Gamma^\alpha_{\mathrm{SLA}} \right\}, \tag{24}$$

consequently

$$\hat{s}\left(\boldsymbol{x}\right) = \hat{s}\left(\boldsymbol{x}\right) + 1 : \forall \boldsymbol{x} \in \Gamma^k_{\mathrm{crit}}. \tag{25}$$

The incremental change of the internal state $\hat{s}\left(\boldsymbol{x}\right)$ and the state variable $\hat{\omega}^k\left(\boldsymbol{x}\right)$ corresponds with energy dissipation

$$\Delta \mathcal{D}^p\left(k\right) = \int_{\Gamma^k_{\mathrm{crit}}} \Delta d\left(\hat{s}\left(\boldsymbol{x}\right)\right) \mathrm{d}\Omega. \tag{26}$$

The above described process of the incremental changes of admissible states $\hat{s}\left(\boldsymbol{x}\right)$ and limited number of discretized states impose next restrictions (in addition to (20)) on the choice of amount of a dissipated energy density as follows

$$\Delta d\left(\hat{s}\left(\boldsymbol{x}\right)\right) = \begin{cases} \text{finite value} : \forall \hat{s}\left(\boldsymbol{x}\right) < q \\ \infty : \forall \hat{s}\left(\boldsymbol{x}\right) = q \end{cases}. \tag{27}$$

3.5 Approximated Energetic Solution

During the construction of the countable set $\mathbb{W}^p$, in each linear analysis, values of all energetic functionals contained in conditions (16) and (17) are quantified. Based on these values, a selection of the energetically admissible states in each time step t^k, which satisfy conditions (16) and (17), is only a question of a postprocessing.

4 Numerics

In this Section, a numerical solution of k-th linear analysis corresponding with minimization problem (21) is introduced.

4.1 Approximation of State Variables

Following the standard Finite Element discretization, each domain is subdivided into simplex elements of a maximum diameter h. Then, the domain displacements receive the form [14]

$$\hat{\boldsymbol{u}}^{(i)}\left(\boldsymbol{x}\right) \approx \hat{\boldsymbol{u}}^{(i)}_h\left(\boldsymbol{x}\right) = \boldsymbol{N}^{(i)}_{u,h}\left(\boldsymbol{x}\right) \hat{\boldsymbol{u}}^{(i)}_h, \qquad \hat{\boldsymbol{u}}_h = \left(\hat{\boldsymbol{u}}^{(1)\mathrm{T}}_h, \hat{\boldsymbol{u}}^{(2)\mathrm{T}}_h, \ldots, \hat{\boldsymbol{u}}^{(n)\mathrm{T}}_h\right)^{\mathrm{T}}, \tag{28}$$

where $\boldsymbol{N}^{(i)}_{u,h}\left(\boldsymbol{x}\right)$ denotes the matrix of basis functions associated with the displacements field and $\hat{\boldsymbol{u}}^{(i)}_h$ are associated nodal displacements, both over i-th domain. The

vector $\hat{\boldsymbol{u}}_h$ collects nodal displacement from all domains. Then, an approximation of the linearized strains over i-th domain is expressed as

$$\hat{\boldsymbol{\epsilon}}^{(i)}(\boldsymbol{x}) \approx \hat{\boldsymbol{\epsilon}}_h^{(i)}(\boldsymbol{x}) = \boldsymbol{B}_{u,h}^{(i)}(\boldsymbol{x})\,\hat{\boldsymbol{u}}_h^{(i)}, \tag{29}$$

where $\boldsymbol{B}_{u,h}^{(i)}(\boldsymbol{x})$ denotes the geometric matrix [14] containing relevant derivatives of the basis functions. The admissible displacement jumps are discretized analogously, so

$$\hat{[\![\boldsymbol{u}]\!]}(\boldsymbol{x}) \approx \hat{[\![\boldsymbol{u}]\!]}_h(\boldsymbol{x}) = \boldsymbol{N}_{[\![u]\!],h}(\boldsymbol{x})\,\hat{[\![\boldsymbol{u}]\!]}_h. \tag{30}$$

Finally, for simplicity, let the partitioning to the finite elements on interfaces is equivalent to the subdivision to the subdomains $\Gamma_{\mathrm{SLA}}^{\alpha}$, than discretization of the damage parameter $\hat{\omega}(\boldsymbol{x})^k$ is automaticaly done by process of SLA, where constant basis functions are used, then

$$\hat{\omega}^k(\boldsymbol{x}) = \hat{\omega}_h^k(\boldsymbol{x}). \tag{31}$$

4.2 Admissible Sets

The set of admissible nodal displacements

$$\mathbb{K}_h^{(i)} = \left\{ \hat{\boldsymbol{u}}_h^{(i)} \in \mathbb{R}^{d\cdot m^{(i)}}, \mathcal{B}_{h,D}^{(i)} \hat{\boldsymbol{u}}_h^{(i)} = \boldsymbol{u}_{h,D}^{(i)} \right\} \tag{32}$$

is defined with regard to corresponding original set (3), where $m^{(i)}$ denotes the number finite element nodes at the i-th domain and the Boolean matrix $\mathcal{B}_{h,D}$ selects the degrees of freedom related to the Dirichlet boundary conditions $\boldsymbol{u}_{h,D}^{(i)}$. The displacement jumps at m interfacial nodes are constrained to the set

$$\mathbb{K}_h^{[\![u]\!]}(\hat{\boldsymbol{u}}_h) = \left\{ \hat{[\![\boldsymbol{u}]\!]}_h \in \mathbb{R}^{d\cdot m}, \mathcal{B}_h^{(i)} \hat{\boldsymbol{u}}_h^{(i)} = \hat{[\![\boldsymbol{u}]\!]}_h, \hat{[\![\boldsymbol{u}]\!]}_{\mathrm{n},h} \geq \boldsymbol{0} \right\}, \tag{33}$$

with $\mathcal{B}_h^{(i)}$ storing the corresponding entries of transformation matrices appearing in (5). Finally, with a view to (31), the discretized set of admissible damage variables satisfies

$$\mathbb{W}_h = \mathbb{W}^p. \tag{34}$$

4.3 Discrete Form of Minimization Problem

Now, a full discrete form of the k-th step of SLA (21) is formulated as

$$(\boldsymbol{u}_{k,h}, [\![\boldsymbol{u}]\!]_{k,h}) = \arg \min_{\left(\hat{\boldsymbol{u}}_h, \hat{[\![\boldsymbol{u}]\!]}_h\right) \in \mathbb{K}_h \times \mathbb{K}_h^{[\![u]\!]}(\boldsymbol{u}_h)} \Phi_{k,h}\left(\hat{\boldsymbol{u}}_h, \hat{[\![\boldsymbol{u}]\!]}_h\right), \tag{35}$$

where the discretized energetic functional has form

$$\begin{aligned} \Phi_{k,h}\left(\hat{\boldsymbol{u}}_h, \hat{[\![\boldsymbol{u}]\!]}_h\right) &= \frac{1}{2}\sum_{i=1}^{n} \hat{\boldsymbol{u}}_h^{(i)\mathrm{T}} \boldsymbol{K}_h^{(i)} \hat{\boldsymbol{u}}_h^{(i)} + \frac{1}{2} \hat{[\![\boldsymbol{u}]\!]}_h{}^{\mathrm{T}} \boldsymbol{K}_h^{\mathrm{int}}\left(\hat{\omega}_h^{k-1}\right) \hat{[\![\boldsymbol{u}]\!]}_h \\ &- \sum_{i=1}^{n} \hat{\boldsymbol{u}}_h^{(i)\mathrm{T}} \boldsymbol{f}_h^{(i)} \end{aligned} \tag{36}$$

The terms appearing in (36) are the stiffness matrix of the i-th domain

$$\boldsymbol{K}_h^{(i)} = \int_{\Omega^{(i)}} \boldsymbol{B}_{u,h}^{(i)\,\mathrm{T}}(\boldsymbol{x})\, \boldsymbol{C}^{(i)}(\boldsymbol{x})\, \boldsymbol{B}_{u,h}^{(i)}(\boldsymbol{x})\, \mathrm{d}\Omega, \tag{37}$$

the vector of reference forces on the i-th domain at unit time

$$\boldsymbol{f}_h^{(i)} = \int_{\Omega^{(i)}} \boldsymbol{N}_{u,h}^{(i)\,\mathrm{T}}(\boldsymbol{x})\, \boldsymbol{v}^{(i)}(1,\boldsymbol{x})\, \mathrm{d}\Omega + \int_{\Gamma^{(i)}} \boldsymbol{N}_{u,h}^{(i)\,\mathrm{T}}(\boldsymbol{x})\, \boldsymbol{t}^{(i)}(1,\boldsymbol{x})\, \mathrm{d}\Gamma \tag{38}$$

and the interfacial stiffness matrix

$$\boldsymbol{K}_h^{\mathrm{int}}\left(\hat{\omega}_h^{k-1}\right) = \int_{\Gamma_{\mathrm{int}}} \frac{G_{c,0}(\boldsymbol{x})}{\Delta^2(\boldsymbol{x})} \left(\frac{1}{\boldsymbol{N}_{\omega,h}(\boldsymbol{x})\, \hat{\omega}_h^{k-1}} - 1 \right) \boldsymbol{N}_{[\![u]\!],h}^{\mathrm{T}}(\boldsymbol{x})\, \boldsymbol{\beta}(\boldsymbol{x})\, \boldsymbol{N}_{[\![u]\!],h}(\boldsymbol{x})\, \mathrm{d}\Gamma. \tag{39}$$

5 FETI-based Solver

5.1 Lagrange function

The Lagrangian function associated with the minimization problem (35) is formed as follows

$$\begin{aligned} L_{k,h}\left(\hat{\boldsymbol{u}}_h, \hat{[\![\boldsymbol{u}]\!]}_h, \hat{\boldsymbol{\lambda}}_h\right) &= \frac{1}{2}\sum_{i=1}^{n} \hat{\boldsymbol{u}}_h^{(i)\mathrm{T}} \boldsymbol{K}_h^{(i)} \hat{\boldsymbol{u}}_h^{(i)} + \frac{1}{2} \hat{[\![\boldsymbol{u}]\!]}_h^{\mathrm{T}} \boldsymbol{K}_h^{\mathrm{int}}\left(\hat{\omega}_h^{k-1}\right) \hat{[\![\boldsymbol{u}]\!]}_h \\ &- \sum_{i=1}^{n} \hat{\boldsymbol{u}}_h^{(i)\mathrm{T}} \boldsymbol{f}_h^{(i)} + \hat{\boldsymbol{\lambda}}_h{}^{\mathrm{T}} \left(\sum_{i=1}^{n} \mathcal{B}_h^{(i)} \hat{\boldsymbol{u}}_h^{(i)} - \hat{[\![\boldsymbol{u}]\!]}_h \right), \end{aligned} \tag{40}$$

where the vector of the nodal Lagrange multipliers $\hat{\boldsymbol{\lambda}}_h$ represents the nodal forces enforcing the geometrical compatibility. Observe that the domain displacements and interfacial displacements jumps become independent. The admissible sets read as

$$\mathbb{L} = \mathbb{R}^{d\cdot m}, \qquad \mathbb{K}_L^{[\![u]\!]} := \left\{ \hat{[\![\boldsymbol{u}]\!]}_h \in \mathbb{R}^{d\cdot m} : \hat{[\![\boldsymbol{u}]\!]}_{\mathrm{n},h} \geq \boldsymbol{0} \right\}. \tag{41}$$

5.2 Stationary Conditions

Note that the inequality in (41) will be enforced by a simple projection technique; the optimality conditions of (40) thus attain the form

$$\frac{\partial L_{k,h}}{\partial \hat{\boldsymbol{u}}_h^{(i)}} = \boldsymbol{K}_h^{(i)} \boldsymbol{u}_{k,h}^{(i)} - \boldsymbol{f}_h^{(i)} + \mathcal{B}_h^{(i)\mathrm{T}} \boldsymbol{\lambda}_{k,h} = \boldsymbol{0}, \tag{42}$$

$$\frac{\partial L_{k,h}}{\partial \hat{\boldsymbol{\lambda}}_h} = \sum_{i=1}^{n} \mathcal{B}_h^{(i)} \boldsymbol{u}_{k,h}^{(i)} - [\![\boldsymbol{u}]\!]_{k,h} = \boldsymbol{0}, \tag{43}$$

$$\frac{\partial L_{k,h}}{\partial \hat{[\![\boldsymbol{u}]\!]}_h} = \boldsymbol{K}_h^{\mathrm{int}}\left(\omega_h^{k-1}\right) [\![\boldsymbol{u}]\!]_{k,h} - \boldsymbol{\lambda}_{k,h} = \boldsymbol{0}. \tag{44}$$

where $i \in \{1, 2, \ldots, n\}$.

5.3 FETI-based Dualization

Now we proceed with the elimination of the primary variables $\boldsymbol{u}_{k,h}^{(i)}$ and $[\![\boldsymbol{u}]\!]_{k,h}$ to express the problem in terms of the dual variables – Lagrange multipliers $\boldsymbol{\lambda}_{k,h}$. To that end, the field of displacements $\boldsymbol{u}_{k,h}^{(i)}$ is expressed in the form

$$\boldsymbol{u}_{k,h}^{(i)} = \boldsymbol{K}_h^{(i)\dagger}\left(\boldsymbol{f}_h^{(i)} - \mathcal{B}_h^{(i)\mathrm{T}}\boldsymbol{\lambda}_{k,h}\right) + \boldsymbol{R}_h^{(i)}\boldsymbol{\alpha}_{k,h}^{(i)}. \tag{45}$$

The first term in relation (45) corresponds to the particular solution of the i-th system (42), expressed by means of the generalized inverse matrix $\boldsymbol{K}_h^{(i)\dagger}$ replacing the inverse matrix for singular $\boldsymbol{K}_h^{(i)}$. The second term in (45) corresponds to a homogeneous solution of the system (42), which is expressed as the linear combination of rigid body motions $\boldsymbol{R}_h^{(i)}$ with coefficients of the linear combination $\boldsymbol{\alpha}_{k,h}^{(i)}$.

When introducing the primary variables (45) into the stationary condition (43), we receive

$$\boldsymbol{F}_h\boldsymbol{\lambda}_{k,h} + \boldsymbol{G}_h\boldsymbol{\alpha}_{k,h} = \boldsymbol{g}_h - [\![\boldsymbol{u}]\!]_{k,h}, \tag{46}$$

where $\boldsymbol{F}_h$ is the compliance matrix of a perfect interface, containing only the domain contributions:

$$\boldsymbol{F}_h = \sum_{i=1}^{n} \mathcal{B}_h^{(i)}\boldsymbol{K}_h^{(i)\dagger}\mathcal{B}_h^{(i)\mathrm{T}} \tag{47}$$

and the remaining terms are provided by

$$\boldsymbol{G}_h = \left(-\mathcal{B}_h^{(1)}\boldsymbol{R}_h^{(1)}, -\mathcal{B}_h^{(2)}\boldsymbol{R}_h^{(2)}, \ldots, -\mathcal{B}_h^{(i)}\boldsymbol{R}_h^{(n)}\right) \tag{48}$$

and

$$\boldsymbol{g}_h = \sum_{i=1}^{n} \mathcal{B}_h^{(i)}\boldsymbol{K}_h^{(i)\dagger}\boldsymbol{f}_h^{(i)}. \tag{49}$$

Equation (46) is an extension of the well-known dual formulation of the original FETI method. To account for additional compliance of an imperfect interface, the displacement jumps are directly related to the Lagrange multipliers via (43), so

$$[\![\boldsymbol{u}]\!]_{k,h} = \left(\boldsymbol{K}_h^{\mathrm{int}}\left(\omega_h^{k-1}\right)\right)^{-1}\boldsymbol{\lambda}_{k,h} = \boldsymbol{H}_{k,h}^{\mathrm{int}}\left(\omega_h^{k-1}\right)\boldsymbol{\lambda}_{k,h}, \tag{50}$$

where the matrix $\boldsymbol{H}_{k,h}^{\mathrm{int}}\left(\omega_h^{k-1}\right)$ is a compliance matrix of interfaces. Altogether, this yields a system of interfacial equations, cf. [9],

$$\left(\boldsymbol{F}_h + \boldsymbol{H}_{k,h}^{\mathrm{int}}\left(\omega_h^{k-1}\right)\right)\boldsymbol{\lambda}_{k,h} + \boldsymbol{G}_h\boldsymbol{\alpha}_{k,h} = \boldsymbol{g}_h. \tag{51}$$

The discrete model is closed by the solvability conditions

$$\boldsymbol{G}_h^{\mathrm{T}}\boldsymbol{\lambda}_{k,h} = \boldsymbol{e}_{h,k}, \tag{52}$$

where

$$\boldsymbol{e}_h^{\mathrm{T}} = \left(\left(-\boldsymbol{R}_h^{(1)\mathrm{T}}\boldsymbol{f}_h^{(1)}\right)^{\mathrm{T}}, \left(-\boldsymbol{R}_h^{(2)\mathrm{T}}\boldsymbol{f}_h^{(2)}\right)^{\mathrm{T}}, \ldots, \left(-\boldsymbol{R}_h^{(n)\mathrm{T}}\boldsymbol{f}_h^{(n)}\right)^{\mathrm{T}}\right). \tag{53}$$

The resulting system can now be efficiently solved using projected Conjugate Gradient algorithm; see, e.g., [10] for additional details.

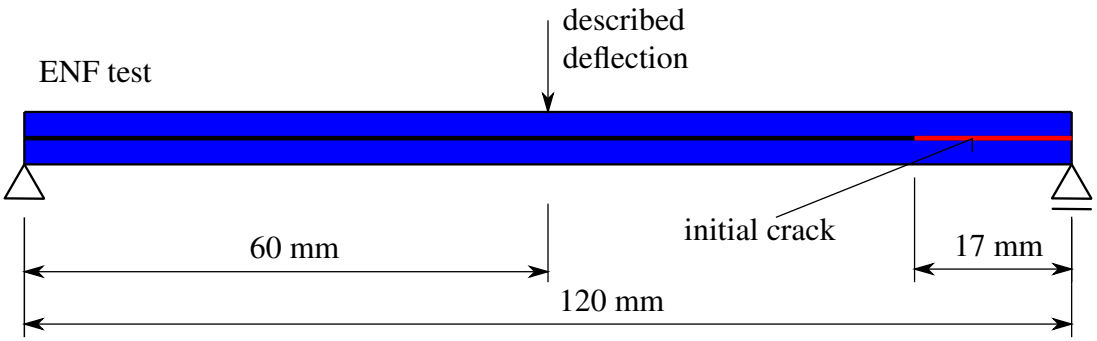

Figure 1: Geometry of specimen.

6 Numerical Experiment

The numerical model presented in the previous sections is implemented in the MATLAB. In particular, a simple two-layer laminated beam with a span of 120 mm was considered, composed of two 3 mm thick and 20 mm wide aluminium layers bonded with adhesive layer. So-called end-notched flexure (ENF) test, commonly used for obtaining pure mode-II loading conditions, is used. In the test, the beam is subjected to a proportional-in-time displacement control bending with a three-point fixtures as shown in Figure 1.

The corresponding material data of the aluminium layers are gathered in Table 1, whereas the interfacial parameters appear in Table 2. The structure was discretized using a regular structural mesh consisting of isoparametric bilinear 4-node plane strain elements with size of 1×1 mm. The obtained load-deflection response is plotted in Figure 2.

Young's modulus, E	75 GPa
Possion's ratio, ν	0.3

Table 1: Material data of the aluminium layers.

fracture toughness, G_c	0.1 N/mm
initial damage, ω_0	0.4
critical stress, $\sigma_{\max}$	8 MPa
critical opening, Δ	0.025 mm
mode mixity parameter, β	1
number of discrete states in material point, q	30

Table 2: Interfacial material data.

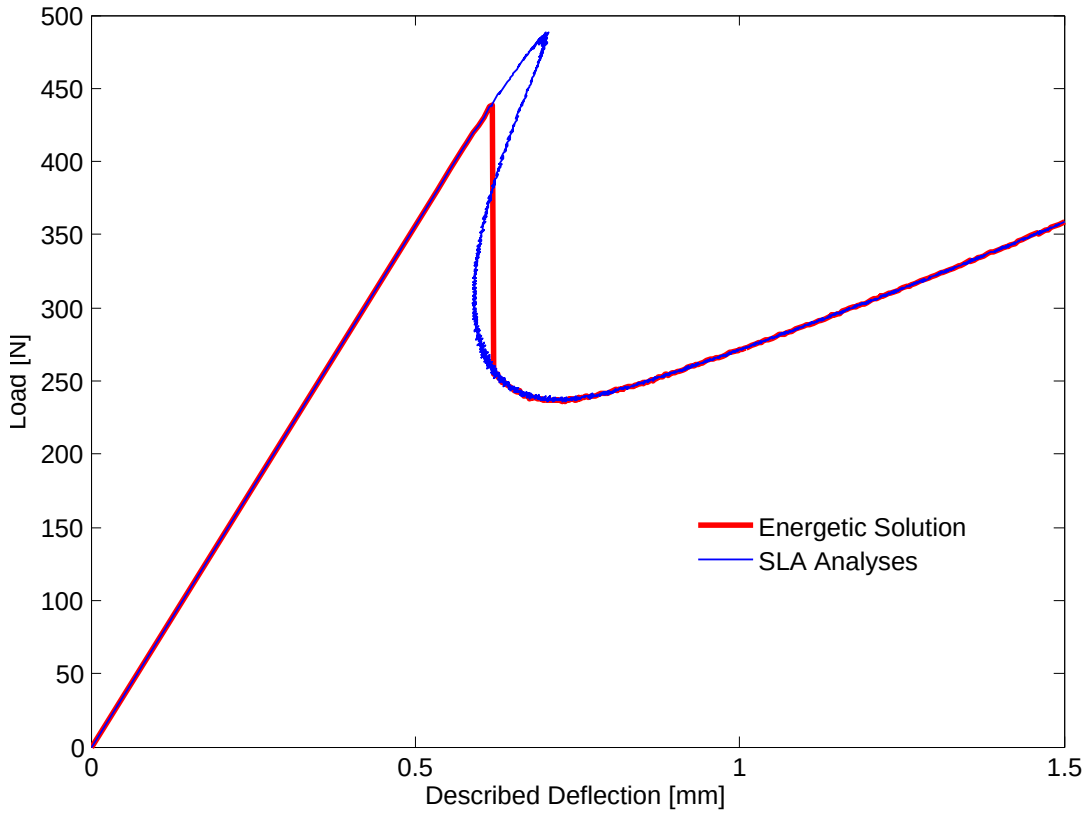

Figure 2: Load-deflection response of ENF test.

7 Conclusion

In the present contribution, a variational approach to simulation of macroscopic delamination of composite structures with quasi-brittle interfaces based on global energy minimization using SLA method has been presented and efficiently resolved by the FETI method. The model consistently incorporates a mixed-mode linear interfacial softening and frictionless contact conditions. As a proof-of-concept for this approach, one numerical example of a two-layered laminated beam failing due to mode-II and characterized by snap-back behaviour was presented.

Acknowledgements

This work was supported by the Czech Science Foundation, under project
No. GA 103/09/H078.

References

[1] A. Orifici, I. Herszberg, R. Thomson, "Review of methodologies for composite material modelling incorporating failure", *Composite Structures*, 86(1–3): 194–210, 2008.

[2] A. Hillerborg, M. Modeer, P. Petersson, "Analysis of crack formation and crack growth in concrete by means of fracture mechanics and finite elements", *Cement and Concrete Research*, 6(6): 773–781, 1976.

[3] P.M.A. Areias, T. Rabczuk, "Quasi-static crack propagation in plane and plate structures using set-valued traction-separation laws", *International Journal for Numerical Methods in Engineering*, 74(3): 475–505, 2008.

[4] Z. Dostál, *Optimal Quadratic Programming Algorithms: With Applications to Variational Inequalities (Springer Optimization and Its Applications)*, Springer, 2009.

[5] M. Kocvara, A. Mielke, T. Roubicek, "A Rate-Independent Approach to the Delamination Problem", *Mathematics and Mechanics of Solids*, 11(4): 423–447, 2006.

[6] P.H. Geubelle, J.S. Baylor, "Impact-induced delamination of composites: a 2D simulation", *Composites Part B: Engineering*, 29(5): 589–602, 1998.

[7] M. Ortiz, A. Pandolfi, "Finite-deformation irreversible cohesive elements for three-dimensional crack-propagation analysis", *International Journal for Numerical Methods in Engineering*, 44(9): 1267–1282, 1999.

[8] C. Farhat, F.X. Roux, "A method of finite element tearing and interconnecting and its parallel solution algorithm", *International Journal for Numerical Methods in Engineering*, 32(6): 1205–1227, 1991.

[9] J. Kruis, Z. Bittnar, "Reinforcement-Matrix Interaction Modeled by FETI Method", in *Domain Decomposition Methods in Science and Engineering XVII*, pages 567–573. Springer, 2008.

[10] J. Kruis, *Domain Decomposition Methods for Distributed Computing*, Saxe-Coburg Publications, 2007.

[11] K. Rektorys, *The Method of Discretization in Time and Partial Differential Equations (Mathematics and its Applications)*, Springer, 1 edition, Dec. 31, 1982, ISBN 9027713421.

[12] A. Mielke, *Chapter 6 Evolution Of Rate-Independent Systems*, Volume 2 of *Handbook of Differential Equations: Evolutionary Equations*, pages 461–559, Elsevier, 2006, ISBN 9780444520487, ISSN 18745717.

[13] J.G. Rots, S. Invernizzi, "Regularized sequentially linear saw-tooth softening model", *Int. J. Numer. Anal. Meth. Geomech.*, 28(7-8): 821–856, 2004.

[14] Z. Bittnar, J. Sejnoha, *Numerical Methods in Structural Mechanics*, American Society of Civil Engineers, 1996.